Physical Communication ▮ (▮▮▮▮) ▮▮▮–▮▮▮

Contents lists available at ScienceDirect

Physical Communication

journal homepage: www.elsevier.com/locate/phycom

Full length article

Orthogonal bi-pulse UWB: Timing and (de)modulation

Mourad Ouertani [a,d], Huilin Xu [b], Hichem Besbes [c], Liuqing Yang [b,*], Ammar Bouallègue [d]

[a] Institut Supérieur d'Informatique, ISI, Tunisia

[b] Department of Electrical & Computer Engr., University of Florida, Gainesville, FL 32601, United States

[c] Research Unit TECHTRA, Ecole Supérieure des Communications de Tunis, Sup'Com, Tunisia

[d] Laboratoire SysCom, Ecole Nationale d'Ingénieurs de Tunis, ENIT, Tunisia

ARTICLE INFO

Keywords:
Ultra-wideband
Orthogonal pulse
Synchronization
Demodulation
Noncoherent

ABSTRACT

In this paper, we propose a novel orthogonal bi-pulse ultra-wideband (UWB) system, which uses an even pulse and an odd pulse to convey information symbols in an alternating manner. Due to the orthogonality of these pulses, their corresponding received waveforms remain orthogonal after propagating through multipath channels. Then we consider two major challenges in the realization of our proposed UWB system: timing synchronization and symbol demodulation. In particular, the idea of timing with dirty template (TDT) in [L. Yang, G.B. Giannakis, Timing Ultra-Wideband signals with dirty templates, IEEE Trans. on Commun. 53 (11) (2005) 1952–1963] is employed for timing synchronization and the noncoherent scheme in [L. Yang, G.B. Giannakis, A. Swami, Noncoherent Ultra-Wideband (de)modulation, IEEE Trans. Commun. 55 (4) (2007) 810–819] is used to bypass channel estimation. Both of these techniques are characterized by correlating adjacent waveform segments. In the implementation of these techniques, we will gradually reveal the advantages of our proposed system. The correlation of adjacent waveform segments only contains the information of a single symbol. This enables a significant enhancement of the synchronization speed of TDT when no training sequence is transmitted. For the same reason, our demodulation approach completely mitigates the inter-symbol interference (ISI) in the second paper referred to, above, and entails a simple demodulator even in the presence of unknown timing errors. Simulations are also carried out to corroborate our analysis.

1. Introduction

Ultra-Wideband (UWB) impulse radios (IR) are carrierless systems, based on the transmission of pulses with very short duration. Due to its huge bandwidth and low power, IR can potentially provide high data-rate transmission in short-range applications, without inducing strong interferences to legacy wireless systems.

Pulse-shape modulation (PSM) has been proposed for UWB IR as a supplement to the traditional pulse-amplitude modulation (PAM) and pulse-position modulation (PPM). By using multiple orthogonal pulses for information transmission, PSM can improve the spectral efficiency when jointly deployed with PAM and PPM (see e.g., [3–5]). In this paper, instead of using multiple pulses for data-rate enhancement, we adopt a pair of orthogonal pulses, an odd waveform and an even waveform, for UWB IR systems to facilitate faster timing synchronization and lower-complexity demodulation.

Timing synchronization is a major challenge in UWB systems (see [6] and the references therein). In [1], timing with dirty template (TDT) was developed for fast synchronization of UWB signals. This technique relies on

* Corresponding address: Department of Electrical & Computer Engineering, University of Florida, P.O.Box 116130, 32601 Gainesville, FL, United States. Tel.: +1 352 392 9469; fax: +1 352 392 0044.

E-mail addresses: ouertani.mourad@gmail.com (M. Ouertani), xuhl@ufl.edu (H. Xu), hichem.besbes@supcom.rnu.tn (H. Besbes), lqyang@ece.ufl.edu (L. Yang), ammar.bouallegue@enit.rnu.tn (A. Bouallègue).

1874-4907/$ – see front matter © 2008 Elsevier B.V. All rights reserved.
doi:10.1016/j.phycom.2008.10.001

correlating adjacent symbol-long segments of the received waveform. TDT is operational with arbitrary and unknown transmitted symbol sequences. When training symbols (pilots) are affordable, the performance of the TDT synchronizer can be improved by adopting a data-aided (DA) mode [1]. The DA mode considerably outperforms the non-data-aided (NDA) one. However, the training sequence entails an overhead which reduces the bandwidth and energy efficiency.

In this paper, we apply the concept of TDT to our proposed orthogonal bi-pulse UWB IR. Similar to the original TDT [1], our timing algorithm also relies on correlating adjacent waveform segments. In particular, a synchronization will be asserted when the correlation function reaches its maximum. Due to the employment of orthogonal pulses, the bi-pulse based TDT can avoid the random symbol effect of the original NDA TDT. Therefore, the bi-pulse TDT can improve the synchronization speed and simultaneously preserve the energy efficiency by only slightly increasing the transceiver complexity.

Due to the extremely rich multipath of UWB channels, channel estimation becomes another big challenge in the realization of the optimal coherent receiver, i.e. the RAKE receiver. Therefore, alternative techniques have been proposed to bypass the explicit channel estimation. These include the transmitted reference (TR) technique [10] which demodulates by correlating the received waveform of each information-bearing symbol with that of an associating pilot symbol, and the differential UWB [11] which correlates the consecutive differentially modulated waveform pair. Operations of these systems require different levels of timing synchronization. However, performance of both degrades when timing error is present. This is because mistiming induces inter-symbol interference (ISI), while the methods in [10,11] both ignore the ISI. Instead of ignoring the ISI, a noncoherent approach is proposed in [2] to explicitly deal with the ISI using Viterbi algorithm, so that maximum likelihood (ML) demodulation of differentially modulated UWB signals becomes possible even in the presence of unknown timing errors.

In this paper, we also employ the noncoherent demodulation algorithm for the orthogonal bi-pulse UWB IR. At the receiver, we use the correlation between neighboring waveform segments for demodulation. Similar to TR UWB and other techniques, our approach remains operational when channel estimation is bypassed. In addition, by using orthogonal pulses, our noncoherent algorithm completely avoids ISI even in the presence of timing errors. As a result, our algorithms only entail a very simple demodulator, while retaining the ML optimality.

Both the timing synchronization and symbol demodulation can be realized in a framework characterized by the extraction and correlation of symbol-level waveforms. Thanks to our novel use of the orthogonal pulse pair, both algorithms can be realized in a more effective manner than the original IR. The rest of this paper is organized as follows. Section 2 describes the bi-pulse UWB IR system model. In Sections 3 and 4, the timing and demodulation algorithms are introduced, respectively. In Section 5, simulations are carried out to corroborate our analysis. Conclusions are given in Section 6.

2. Bi-pulse UWB impulse radio

In this section, we will first introduce the system model for conventional UWB IRs. Then, we will extend this model to a bi-pulse IR system by replacing the single pulse shaper with a pair of orthogonal pulses.

2.1. Conventional UWB impulse radio

Let us consider an IR UWB system, where each information symbol is transmitted over a T_s period that consists of N_f frames. During each frame of duration T_f, a data-modulated pulse $p(t)$ with duration $T_p \ll T_f$ is transmitted from the antenna. The transmitted signal is

$$v(t) = \sqrt{\mathcal{E}} \sum_{n=0}^{\infty} \tilde{s}(n) \cdot p_T(t - nT_s) \tag{1}$$

where $\mathcal{E}$ is the energy per pulse, $\tilde{s}(n) := s(n)\tilde{s}(n-1)$ are differentially encoded symbols with $s(n)$ denoting the binary PAM information symbols and $p_T(t)$ denotes the symbol-level transmitted waveform:

$$p_T(t) = \sum_{n=0}^{N_f-1} c_{ds}(n) \cdot p(t - nT_f - c_{th}(n)T_c) \tag{2}$$

where T_c is the chip duration. Notice that $p_T(t)$ can be regarded as the symbol-level pulse shaper which accounts for the time-hopping (TH) and/or direct-sequence (DS) spreading via $c_{th}(n)$ and $c_{ds}(n)$, respectively.

The transmitted signal propagates through the multipath channel with impulse response

$$g(t) = \sum_{l=0}^{L-1} \alpha_l \delta(t - \tau_l) \tag{3}$$

where $\{\alpha_l\}_{l=0}^{l=L-1}$ and $\{\tau_l\}_{l=0}^{l=L-1}$ are amplitudes and delays of the L multipath elements, respectively. Among $\{\tau_l\}_{l=0}^{l=L-1}$, τ_0 represents the propagation delay of the channel.

Then, the received waveform is given by

$$r(t) = \sqrt{\mathcal{E}} \sum_{n=0}^{\infty} \tilde{s}(n) \cdot p_R(t - nT_s - \tau_0 + \tau_r) + \eta(t) \tag{4}$$

where $\eta(t)$ is the additive noise, τ_r is arbitrary reference at the receiver and $p_R(t)$ denotes the aggregate symbol-level received waveform:

$$p_R(t) = \sum_{n=0}^{N_f-1} c_{ds}(n) \cdot p(t - nT_f - c_{th}(n)T_c) * g(t + \tau_0) \tag{5}$$

where $*$ denotes the convolution operation.[1] Let us define $\Delta\tau := \tau_r - \tau_0$ as the timing offset. Without loss of generality, we assume that $\Delta\tau$ is in the range of $[0, T_s)$. As we will show in the rest of this paper, this assumption will not affect the timing synchronization and the differential demodulation.

[1] Due to the distortion effects of transmit and receive antennas, the receive pulse shaper could be different from $p(t)$ [18]. However, this will not affect the design and operation of our bi-pulse timing synchronizer and demodulator in this paper.

Please cite this article in press as: M. Ouertani, et al., Orthogonal bi-pulse UWB: Timing and (de)modulation, Physical Communication (2008), doi:10.1016/j.phycom.2008.10.001

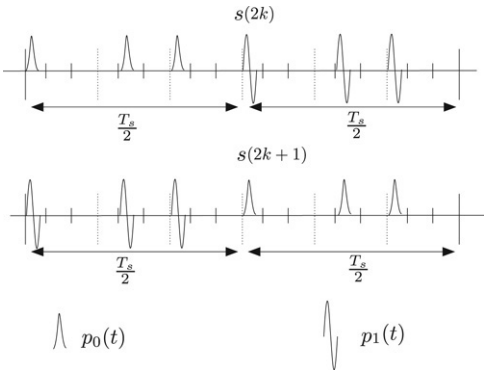

Fig. 1. Transmitted waveforms using orthogonal modulation scheme and the TH code [0, 1, 0].

2.2. Bi-pulse IR system model

In our system, every encoded information symbol is still transmitted over a T_s duration. However, each symbol duration is divided into two equal halves. The two halves will use a pair of pulse shapers: an even waveform $p_0(t)$ and an odd waveform $p_1(t)$. The even and odd pulses can be chosen as Gaussian pulses [7], Hermite pulses [13], or their derivatives. The optimal design of these pulses has been widely investigated in the literature (see e.g., [8,9]).

For the symbol with an even index, the pulse $p_0(t)$ is data-modulated and transmitted in the first half of the symbol duration and pulse $p_1(t)$ in the second half. For the symbol with an odd index, $p_1(t)$ is used for the former half and $p_0(t)$ for the latter half of the symbol duration (see Fig. 1). For this approach, we use the same time-hopping and spreading codes for the two halves, i.e., $c_{th}(i) = c_{th}(N_f/2+i)$ and $c_{ds}(i) = c_{ds}(N_f/2+i)$, $i \in [0, N_f/2-1]$.

Denote the symbol-level transmitted waveform with an even index by $p_{T0}(t)$ and by $p_{T1}(t)$ otherwise. The received signal is given by:

$$r(t) = \sqrt{\mathcal{E}} \sum_{n=0}^{\infty} \widetilde{s}(n) \cdot p_{Ri_n}(t - nT_s + \Delta\tau) + \eta(t) \tag{6}$$

where $p_{Ri_n}(t)$ is the noise-free received symbol-level waveform with $i_n = [n]_2$. Here we use $[A]_B$ for the modulo operation with base B. To facilitate the noncoherent UWB demodulation, we select T_f and the TH code of the $(N_f/2-1)$st frame to satisfy $(c_{th}(N_f/2-1)T_c + T_p + \tau_{L-1}) < T_f$ so that there is no interference between the even and odd waveforms ($p_0(t)$ and $p_1(t)$) even after multipath propagation. However, it is worth noting that no constraint is imposed on the inter-frame interference and inter-pulse interference within each $T_s/2$ duration exclusively containing $p_0(t)$ or $p_1(t)$. Then, we can express $p_{R0}(t)$ and $p_{R1}(t)$ as follows:

$$p_{R0}(t) = \begin{cases} R_0(t) & \text{if } t \in \left[0, \frac{T_s}{2}\right) \\ R_1\left(t - \frac{T_s}{2}\right) & \text{if } t \in \left[\frac{T_s}{2}, T_s\right) \end{cases}$$
$$p_{R1}(t) = \begin{cases} R_1(t) & \text{if } t \in \left[0, \frac{T_s}{2}\right) \\ R_0\left(t - \frac{T_s}{2}\right) & \text{if } t \in \left[\frac{T_s}{2}, T_s\right) \end{cases} \tag{7}$$

where

$$R_0(t) = \sum_{n=0}^{N_f/2-1} c_{ds}(n) \cdot p_0(t - nT_f - c_{th}(n)T_c) * g(t + \tau_0)$$

and

$$R_1(t) = \sum_{n=0}^{N_f/2-1} c_{ds}(n) \cdot p_1(t - nT_f - c_{th}(n)T_c) * g(t + \tau_0)$$

denote the parts of symbol-level waveforms involving $p_0(t)$ and $p_1(t)$, respectively.

For illustrative purpose, $R_i(t)$ is plotted in Fig. 2 as a triangle with the maximum non-zero support of $T_s/2$ and the frame-level repetition is ignored. Notice that due to the timing error, every $R_i(t)$ can be partitioned into two segments $q_i^a(t, \Delta\tau)$ and $q_i^b(t, \Delta\tau)$ (see Fig. 2):

$$q_i^a(t, \Delta\tau) = \begin{cases} 0, & t \in \left[0, \frac{T_s}{2} - [\Delta\tau]_{T_s/2}\right) \\ R_i\left(t - \frac{T_s}{2} + [\Delta\tau]_{T_s/2}\right), & \\ & t \in \left[\frac{T_s}{2} - [\Delta\tau]_{T_s/2}, \frac{T_s}{2}\right) \end{cases} \tag{8}$$

and

$$q_i^b(t, \Delta\tau) = \begin{cases} R_i(t + [\Delta\tau]_{T_s/2}), & \\ & t \in \left[0, \frac{T_s}{2} - [\Delta\tau]_{T_s/2}\right) \\ 0, & t \in \left[\frac{T_s}{2} - [\Delta\tau]_{T_s/2}, \frac{T_s}{2}\right). \end{cases} \tag{9}$$

The waveforms $q_i^a(t, \Delta\tau)$ and $q_i^b(t, \Delta\tau)$ constitute the complete waveform $R_i(t)$ as:

$$R_i(t) = q_i^a\left(t + T_s/2 - [\Delta\tau]_{T_s/2}, \Delta\tau\right) + q_i^b\left(t - [\Delta\tau]_{T_s/2}, \Delta\tau\right). \tag{10}$$

Timing synchronization and channel estimation are two major challenges for the realization of UWB IR. In the next two sections, we will discuss how to address these problems for our proposed orthogonal bi-pulse UWB IR system.

3. Timing Bi-pulse UWB signals

In this section, we will derive an NDA timing synchronizer based on the orthogonal bi-pulse UWB system. Following the idea of TDT [1], our timing algorithm also relies on correlating the neighboring signal segments. Instead of taking T_s-long segments, however, TDT for bi-pulse IR relies on half-symbol ($T_s/2$)-long segments of the received waveform.

Our demodulation starts with extracting the $T_s/2$-long segments from the received waveform. These segments are given by:

$$\begin{matrix} r_n(t) = r(t + nT_s) \\ r_n(t + T_s/2) = r(t + nT_s + T_s/2) \end{matrix}, \quad t \in [0, T_s/2). \tag{11}$$

Please cite this article in press as: M. Ouertani, et al., Orthogonal bi-pulse UWB: Timing and (de)modulation, Physical Communication (2008), doi:10.1016/j.phycom.2008.10.001

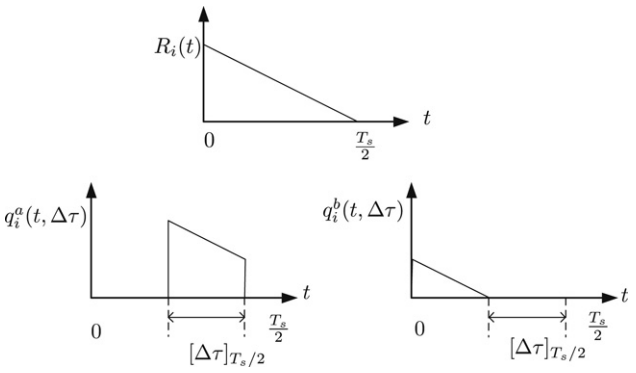

Fig. 2. The $T_s/2$-long signal segments.

Then, adjacent segments are correlated to calculate the correlation function $x(n, \Delta\tau)$:

$$x(n, \Delta\tau) = \int_0^{\frac{T_s}{2}} r_n(t) r_n\left(t - \frac{T_s}{2}\right) \mathrm{d}t. \tag{12}$$

The next question is how to recover the timing offset $\Delta\tau$ from this correlation function.

Let us first introduce two Lemmas which will be used to derive the timing algorithm from Eq. (12).

Lemma 1. *Let $p_0(t)$ and $p_1(t)$ constitute an even and odd pulse pair. After propagating through any real channel, the received waveforms corresponding to $p_0(t)$ and $p_1(t)$ are still orthogonal.*

Proof. See Appendix. □

Lemma 1 implies that

$$\int_0^{\frac{T_s}{2}} q_0^{\alpha}(t, \Delta\tau) q_1^{\alpha}(t, \Delta\tau)\mathrm{d}t = 0, \quad \alpha \in \{a, b\}.$$

In addition, since the non-zero supports of $q_i^a(t, \Delta\tau)$ and $q_i^b(t, \Delta\tau)$ do not overlap, the following always holds true:

Lemma 2. *When the non-zero support of $R_i(t)$ is upper bounded by $T_s/2$, we have*

$$\int_0^{\frac{T_s}{2}} q_i^a(t, \Delta\tau) q_i^b(t, \Delta\tau)\mathrm{d}t = 0, \quad i \in \{0, 1\}. \tag{13}$$

This is evident from Eqs. (8) and (9).

With these results, we are ready to recover the timing error $\Delta\tau$ from the correlation function $x(n, \Delta\tau)$ in Eq. (12). Using Lemmas 1 and 2, $x(n, \Delta\tau)$ can be expressed in a very simple form which contains the energy of either $q_i^a(t)$ or $q_i^b(t)$, $i \in \{0, 1\}$, depending on whether $\Delta\tau \in [0, T_s/2)$ or $\Delta\tau \in [T_s/2, T_s)$.

3.1. Case I: $\Delta\tau \in [0, T_s/2)$

In this case, the noise-free signal segments involved in timing synchronization are [cf. (6) and (11)]

$$\begin{aligned} \bar{r}_n(t - T_s/2) &= \widetilde{s}(n-1) q_i^b(t, \Delta\tau) + \widetilde{s}(n) q_i^a(t, \Delta\tau) \\ \bar{r}_n(t) &= \widetilde{s}(n) q_i^b(t, \Delta\tau) + \widetilde{s}(n) q_j^a(t, \Delta\tau), \\ & i \neq j \in \{0, 1\} \end{aligned} \tag{14}$$

where $\bar{r}_n(t - T_s/2)$ and $\bar{r}_n(t)$ are the noise-free parts of $r_n(t - T_s/2)$ and $r_n(t)$, respectively. As a result, the noise free part of the correlation function $x(n, \Delta\tau)$ can be expressed as [cf. (12)]:

$$\begin{aligned} \bar{x}(n, \Delta\tau) = \int_0^{\frac{T_s}{2}} & \left(\widetilde{s}(n-1) q_i^b(t, \Delta\tau) + \widetilde{s}(n) q_i^a(t, \Delta\tau)\right) \\ & \times \left(\widetilde{s}(n) q_i^b(t, \Delta\tau) + \widetilde{s}(n) q_j^a(t, \Delta\tau)\right) \mathrm{d}t. \end{aligned} \tag{15}$$

Using Lemmas 1 and 2, and the differential modulation relationship, $\bar{x}(n, \Delta\tau)$ becomes:

$$\bar{x}(n, \Delta\tau) = \int_0^{\frac{T_s}{2}} s_n (q_i^b(t, \Delta\tau))^2 \mathrm{d}t. \tag{16}$$

Accordingly, the absolute value of $\bar{x}(n, \Delta\tau)$ can be equivalently expressed as:

$$|\bar{x}(n, \Delta\tau)| = \int_0^{\frac{T_s}{2}} \left(q_i^b(t, \Delta\tau)\right)^2 \mathrm{d}t := \mathcal{E}_b(\Delta\tau) \tag{17}$$

where $\mathcal{E}_b(\Delta\tau)$ is defined as the energy of the waveform segment $q_i^b(t, \Delta\tau)$. In the random channel environment, it is reasonable to assume that $q_0^b(t, \Delta\tau)$ and $q_1^b(t, \Delta\tau)$ approximately have the same energy $\mathcal{E}_b(\Delta\tau)$. It should be noted that $\mathcal{E}_b(\Delta\tau)$ decreases as $\Delta\tau$ increases (see Fig. 2). Therefore, we have the following result:

Proposition 1. *For the orthogonal bi-pulse UWB IR system, when the timing error $\Delta\tau$ is in the range of $[0, T_s/2)$, the absolute value of the noise-free correlation function $|\bar{x}(n, \Delta\tau)|$ equals the energy $\mathcal{E}_b(\Delta\tau)$ of the waveform segment $q_i^b(t, \Delta\tau)$, which is a decreasing function in $\Delta\tau$.*

Notice that Eq. (17) shows that $|\bar{x}(n, \Delta\tau)|$ is a constant independent of the symbol index n, even when a random

symbol sequence is transmitted. This consists of a fundamental difference between our method here and the original TDT in [1], where the correlator output varies with the particular symbol sequence transmitted. As a result, unlike the original TDT in [1] that entails significant averaging or special training patterns to remove the random symbol effect, our approach here completely avoids such a problem.

3.2. Case II: $\Delta\tau \in [T_s/2, T_s)$

In this case, the noise-free signal segments involved in timing are [cf. (6) and (11)]

$$\begin{aligned}\bar{r}_n(t - T_s/2) &= \widetilde{s}(n)q_i^b(t, \Delta\tau) + \widetilde{s}(n)q_j^a(t, \Delta\tau)\\ \bar{r}_n(t) &= \widetilde{s}(n)q_j^b(t, \Delta\tau) + \widetilde{s}(n+1)q_j^a(t, \Delta\tau),\\ & i \neq j \in \{0, 1\}.\end{aligned} \tag{18}$$

The noise-free correlation function can be expressed as [cf. (12)]:

$$\begin{aligned}\bar{x}(n, \Delta\tau) = &\int_0^{T_s} \left(\widetilde{s}(n)q_i^b(t, \Delta\tau) + \widetilde{s}(n)q_j^a(t, \Delta\tau)\right)\\ &\times \left(\widetilde{s}(n)q_j^b(t, \Delta\tau) + \widetilde{s}(n+1)q_j^a(t, \Delta\tau)\right) \mathrm{d}t.\end{aligned} \tag{19}$$

Using Lemmas 1 and 2, $\bar{x}(n, \Delta\tau)$ becomes:

$$\bar{x}(n, \Delta\tau) = \int_0^{\frac{T_s}{2}} s_{n+1}(q_j^a(t, \Delta\tau))^2 \mathrm{d}t. \tag{20}$$

Accordingly, the absolute value of $\bar{x}(n, \Delta\tau)$ can be equivalently expressed as:

$$|\bar{x}(n, \Delta\tau)| = \int_0^{\frac{T_s}{2}} \left(q_j^a(t, \Delta\tau)\right)^2 \mathrm{d}t := \mathcal{E}_a(\Delta\tau) \tag{21}$$

where $\mathcal{E}_a(\Delta\tau)$ is the energy of waveform segment $q_j^a(t, \Delta\tau), j \in \{0, 1\}$. Since $\mathcal{E}_a(\Delta\tau)$ increases as $\Delta\tau$ increases (see Fig. 2), we have the following result:

Proposition 2. *For the orthogonal bi-pulse UWB IR system, when the timing error $\Delta\tau$ is in the range of $[T_s/2, T_s)$, the absolute value of the noise-free correlation function $|\bar{x}(n, \Delta\tau)|$ equals the energy $\mathcal{E}_a(\Delta\tau)$ of the waveform segment $q_j^a(t, \Delta\tau)$, which is an increasing function in $\Delta\tau$.*

Notice that here $|\bar{x}(n, \Delta\tau)|$ also remains a constant $\forall n$, at any given $\Delta\tau$. This again confirms that the random symbol effect is completely mitigated in our bi-pulse IR approach.

3.3. TDT for Bi-pulse IR

Generally, it is unknown to the receiver whether $\Delta\tau$ is in $[0, T_s/2)$ or in $[T_s/2, T_s)$. However, we notice that for $\Delta\tau \in [0, T_s/2)$, $|\bar{x}(n, \Delta\tau)| = \mathcal{E}_b(\Delta\tau)$ increasingly approaches its maximum $\mathcal{E}_b(0) = \mathcal{E}_R$ when $\Delta\tau$ approaches 0; it also decreasingly approaches its minimum $\mathcal{E}_b(T_s/2) = 0$ when $\Delta\tau$ approaches $T_s/2$ (see Fig. 2). In addition, for $\Delta\tau \in [T_s/2, T_s)$, $|\bar{x}(n, \Delta\tau)| = \mathcal{E}_a(\Delta\tau)$ decreasingly approaches its minimum $\mathcal{E}_a(T_s/2) = 0$ when $\Delta\tau$ approaches $T_s/2$ and increasingly approaches its maximum $\mathcal{E}_a(T_s) = \mathcal{E}_R$ when $\Delta\tau$ approaches T_s. Therefore, $|\bar{x}(n, \Delta\tau)|$ is continuous at $\Delta\tau = T_s/2$. Moreover, $|\bar{x}(n, \Delta\tau)|$ is a periodic function of $\Delta\tau$ with period of T_s; that is, $|\bar{x}(n, \Delta\tau)| = |\bar{x}(n, T_s + \Delta\tau)|, \forall\Delta\tau$. Therefore, $|\bar{x}(n, \Delta\tau)|$ reaches its minimum when $\Delta\tau = T_s/2$, and reaches its maximum when $\Delta\tau = 0$. This result leads to a timing synchronizer based on the sample mean of the symbol-rate samples $|x(n, \Delta\tau)|$.

In the following, we combine Propositions 1 and 2 to build a timing synchronizer for our proposed bi-pulse IR system:

Proposition 3. *For the orthogonal bi-pulse IR system, a blind timing synchronizer can be built even when TH codes are present and the UWB multipath channel is unknown. The timing algorithm can be summarized in the following steps:*

Step 1: *Extract the $T_s/2$-long segments $r(t + nT_s)$ and $r(t + nT_s - T_s/2)$ from the received waveform.*

Step 2: *Estimate the noise-free correlation function of adjacent segments with*

$$y(M, \Delta\tau) = \frac{1}{M} \times \sum_{n=1}^{M} \left| \int_0^{\frac{T_s}{2}} r(t + nT_s) r(t + nT_s - T_s/2) \mathrm{d}t \right|.$$

Step 3: *The timing error can be estimated when $y(M, \Delta\tau)$ reaches its maximum*

$$\widehat{\Delta\tau} = \arg \max_{\Delta\tau \in [0, T_s)} y(M, \Delta\tau).$$

Unlike the original NDA TDT, the estimation of the correlation function for our synchronizer is not affected by the ISI (see Eqs. (17) and (21)) even with random information symbols. Therefore, the proposed synchronization approach is expected to achieve a better acquisition performance than that of the original TDT in the NDA mode (see Fig. 3).

4. Demodulating Bi-pulse UWB signals

Following the noncoherent UWB [12], our demodulation also builds on correlating the neighboring signal segments. The advantage is that due to the orthogonality between $p_0(t)$ and $p_1(t)$, our algorithm avoids ISI even in the presence of mistiming. The demodulation algorithm also starts from the extraction and correlation of $T_s/2$-long waveform segments. The extraction is as described in the preceding section. However, the correlation is carried out in a different manner, as detailed in the following.

4.1. Extraction of decision statistics

Instead of $x(n, \Delta\tau)$, we calculate *two* correlation functions $x_1(n, \Delta\tau)$ and $x_2(n, \Delta\tau)$ (see Fig. 4):

$$\begin{aligned}x_1(n, \Delta\tau) = &\int_0^{\frac{T_s}{2}} r_n(t) r_{n-1}\left(t + \frac{T_s}{2}\right) \mathrm{d}t\\ &+ \int_0^{\frac{T_s}{2}} r_n\left(t + \frac{T_s}{2}\right) r_{n-1}(t) \mathrm{d}t\end{aligned} \tag{22}$$

Please cite this article in press as: M. Ouertani, et al., Orthogonal bi-pulse UWB: Timing and (de)modulation, Physical Communication (2008), doi:10.1016/j.phycom.2008.10.001

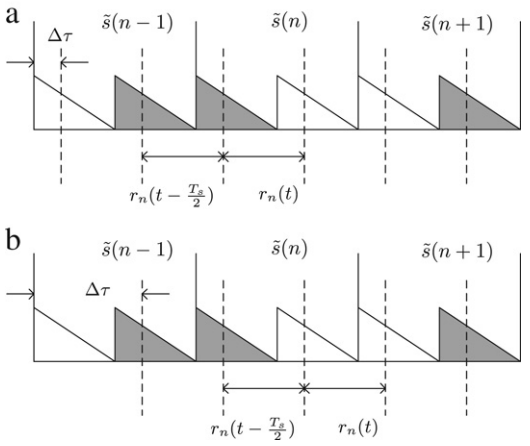

Fig. 3. Timing for noncoherent orthogonal bi-pulse UWB (a) $\Delta\tau \in [0, T_s/2)$, and (b) $\Delta\tau \in [T_s/2, T_s)$.

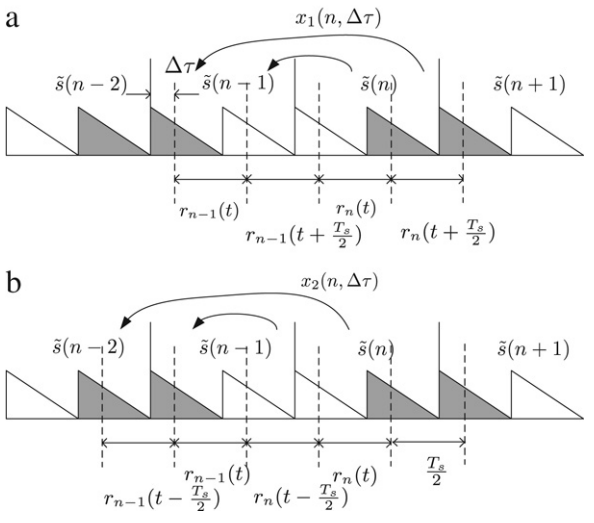

Fig. 4. Demodulation algorithm in the presence of timing error.

$$x_2(n,\Delta\tau) = \int_0^{\frac{T_s}{2}} r_n\left(t-\frac{T_s}{2}\right) r_{n-1}(t)\,dt + \int_0^{\frac{T_s}{2}} r_n(t)\, r_{n-1}\left(t-\frac{T_s}{2}\right) dt. \quad (23)$$

As shown in the following, we use both correlation functions to demodulate one symbol because either of them only contains part of the symbol energy in the presence of mistiming. Using $x_1(n,\Delta\tau)$ and $x_2(n,\Delta\tau)$ together, one can obtain the entire symbol energy from the received waveform.

For $\Delta\tau \in [0, T_s/2)$, signal segments with index n involved in the demodulation are

$$\begin{aligned} r_n(t) &= \tilde{s}(n)q_i^b(t,\Delta\tau) + \tilde{s}(n)q_j^a(t,\Delta\tau) + \eta_1(t) \\ r_n(t-T_s/2) &= \tilde{s}(n-1)q_i^b(t,\Delta\tau) + \tilde{s}(n)q_i^a(t,\Delta\tau) + \eta_2(t) \\ r_n(t+T_s/2) &= \tilde{s}(n)q_j^b(t,\Delta\tau) + \tilde{s}(n+1)q_j^a(t,\Delta\tau) + \eta_3(t) \end{aligned} \quad (24)$$

and segments with index $(n-1)$ are

$$\begin{aligned} r_{n-1}(t) &= \tilde{s}(n-1)q_j^b(t,\Delta\tau) + \tilde{s}(n-1)q_i^a(t,\Delta\tau) + \eta_4(t) \\ r_{n-1}(t-T_s/2) &= \tilde{s}(n-2)q_j^b(t,\Delta\tau) + \tilde{s}(n-1)q_j^a(t,\Delta\tau) + \eta_5(t) \\ r_{n-1}(t+T_s/2) &= \tilde{s}(n-1)q_i^b(t,\Delta\tau) + \tilde{s}(n)q_i^a(t,\Delta\tau) + \eta_6(t). \end{aligned} \quad (25)$$

These notions seem to be rather redundant. However, because the orthogonal pulse pair used in our bi-pulse IR switches in order from symbol to symbol, $r_n(t)$ is different from $r_{n-1}(t)$ since they contain different combinations of $q_i^\alpha(t)$, $i \in \{0,1\}$, $\alpha \in \{a,b\}$, except for that $r_n(t-T_s/2) = r_{n-1}(t+T_s/2)$.

Using Lemmas 1 and 2, correlation functions $x_1(n,\Delta\tau)$ and $x_2(n,\Delta\tau)$ can be simplified to:

$$\begin{aligned} x_1(n,\Delta\tau) &= 2s(n)\mathcal{E}_b(\Delta\tau) + \xi_1(n) \\ x_2(n,\Delta\tau) &= 2s(n)\mathcal{E}_a(\Delta\tau) + \xi_2(n) \end{aligned} \quad (26)$$

where $\mathcal{E}_a(\Delta\tau)$ and $\mathcal{E}_b(\Delta\tau)$ are the energy of waveform segments $q_i^a(t,\Delta\tau)$ and $q_i^b(t,\Delta\tau)$ for $i \in \{0,1\}$ as defined by Eqs. (17) and (21), respectively, and $\xi_1(n)$ as well as $\xi_2(n)$ are noise terms.

From (26), we see that each correlation function only contains the information of one transmitted symbol. This is distinct from the original noncoherent UWB in [2] where the correlation result always contains two consecutive information symbols, when timing error is present. Therefore, due to the orthogonality of the UWB pulses, our noncoherent demodulator avoids the ISI and thus the Viterbi decoding required by [2]. In addition, each symbol $s(n)$ is contained in both $x_1(n,\Delta\tau)$ and $x_2(n,\Delta\tau)$. The noise-free part of $x_1(n,\Delta\tau) + x_2(n,\Delta\tau)$ contains all available energy of one symbol.

Similarly, for $\Delta\tau \in [T_s/2, T_s)$, correlation functions $x_1(n,\Delta\tau)$ and $x_2(n,\Delta\tau)$ can be expressed as:

$$\begin{aligned} x_1(n-1,\Delta\tau) &= 2s(n)\mathcal{E}_a(\Delta\tau) + \xi_3(n-1) \\ x_2(n,\Delta\tau) &= 2s(n)\mathcal{E}_b(\Delta\tau) + \xi_4(n) \end{aligned} \quad (27)$$

where $\xi_3(n)$ and $\xi_4(n)$ are noise terms. Notice that here we consider $x_1(n-1,\Delta\tau)$ instead of $x_1(n,\Delta\tau)$ since the former contains the same symbol as $x_2(n,\Delta\tau)$.

Clearly, to distinguish which of (26) and (27) is the case, one needs to separate the $\Delta\tau \in [0, T_s/2)$ case from the $\Delta\tau \in [T_s/2, T_s)$ case. For a random symbol sequence, these cases can be distinguished by using the following rule:

$\Delta\tau$ is in the range of $[0, T_s/2)$ if

$$\mathrm{E}\{|x_1(n,\Delta\tau) + x_2(n,\Delta\tau)|\} \geq \mathrm{E}\{|x_1(n-1,\Delta\tau) + x_2(n,\Delta\tau)|\} \quad (28)$$

and $\Delta\tau \in [T_s/2, T_s)$ if otherwise.

This can be easily seen from (26) (or (27)) since $x_1(n,\Delta\tau)$ and $x_2(n,\Delta\tau)$ contain the same symbol if $\Delta\tau \in [0, T_s/2)$, while $x_1(n-1,\Delta\tau)$ and $x_2(n,\Delta\tau)$ contain the

Please cite this article in press as: M. Ouertani, et al., Orthogonal bi-pulse UWB: Timing and (de)modulation, Physical Communication (2008), doi:10.1016/j.phycom.2008.10.001

same symbol if $\Delta\tau \in [T_s/2, T_s)$. The expectation can be approximated by

$$\mathrm{E}\{|x_1(n,\Delta\tau)+x_2(n,\Delta\tau)|\} \approx \frac{1}{M}\sum_{n=0}^{M-1}|x_1(n,\Delta\tau)+x_2(n,\Delta\tau)|$$

with M being the length of symbol sequence.

4.2. Symbol detection

Before deriving the decoding algorithm, let us first investigate the statistical distribution of the noise terms in Eqs. (26) and (27). For UWB pulses used in this paper, both the analysis along the lines of [14, Appendix I] and simulations confirm that $\xi_1(n)$ and $\xi_2(n)$ (also $\xi_3(n-1)$ and $\xi_4(n)$) are uncorrelated zero-mean Gaussian random variables with equal variances, for any arbitrary channel realization, symbol sequence and timing error $\Delta\tau \in [0, T_s)$. Based on these, we can combine $x_1(n,\Delta\tau)$ (or $x_1(n-1,\Delta\tau)$) and $x_2(n,\Delta\tau)$ with selective combining (SC), equal gain combining (EGC) or maximal ratio combining (MRC).

For SC, the correlation output with more energy is selected. For $\Delta\tau \in [0, T_s/2)$, the information symbol can be estimated as

$$\widehat{s}(n)=\begin{cases}\mathrm{sign}(x_1(n,\Delta\tau)) & \text{if } \widehat{\mathcal{E}}_b(\Delta\tau)\geq\widehat{\mathcal{E}}_a(\Delta\tau)\\ \mathrm{sign}(x_2(n,\Delta\tau)) & \text{if } \widehat{\mathcal{E}}_a(\Delta\tau)>\widehat{\mathcal{E}}_b(\Delta\tau)\end{cases} \tag{29}$$

where $\widehat{\mathcal{E}}_a(\Delta\tau)$ and $\widehat{\mathcal{E}}_b(\Delta\tau)$ are estimates of the signal strength $\mathcal{E}_a(\Delta\tau)$ and $\mathcal{E}_b(\Delta\tau)$ contained in $x_1(n,\Delta\tau)$ and $x_2(n,\Delta\tau)$:

$$\widehat{\mathcal{E}}_b(\Delta\tau)=\frac{1}{M}\sum_{n=0}^{M-1}|x_1(n,\Delta\tau)|$$
$$\widehat{\mathcal{E}}_a(\Delta\tau)=\frac{1}{M}\sum_{n=0}^{M-1}|x_2(n,\Delta\tau)|\,. \tag{30}$$

Similarly, for $\Delta\tau \in [T_s/2, T_s)$, $s(n)$ can be estimated by

$$\widehat{s}(n)=\begin{cases}\mathrm{sign}(x_1(n-1,\Delta\tau)) & \text{if } \widehat{\mathcal{E}}_a(\Delta\tau)\geq\widehat{\mathcal{E}}_b(\Delta\tau)\\ \mathrm{sign}(x_2(n,\Delta\tau)) & \text{if } \widehat{\mathcal{E}}_b(\Delta\tau)>\widehat{\mathcal{E}}_a(\Delta\tau).\end{cases} \tag{31}$$

For EGC, the two correlation functions are simply added together to obtain the decision statistic. For $\Delta\tau \in (0, T_s/2)$, the information symbol can be estimated by

$$\widehat{s}(n)=\mathrm{sign}(x_1(n,\Delta\tau)+x_2(n,\Delta\tau)) \tag{32}$$

and for $\Delta\tau \in [T_s/2, T_s)$

$$\widehat{s}(n)=\mathrm{sign}(x_1(n-1,\Delta\tau)+x_2(n,\Delta\tau)). \tag{33}$$

For MRC, the two correlation functions are weighted and added together to maximize the signal-to-noise ratio (SNR) of the decision statistic. The optimal weight coefficients of $x_1(n,\Delta\tau)$ and $x_2(n,\Delta\tau)$ are proportional to their signal amplitudes $\mathcal{E}_a(\Delta\tau)$ and $\mathcal{E}_b(\Delta\tau)$, respectively. In practice, estimates of $\mathcal{E}_a(\Delta\tau)$ and $\mathcal{E}_b(\Delta\tau)$ are used as the weight coefficients. Then, for $\Delta\tau \in (0, T_s/2)$, the information symbol can be estimated by

$$\widehat{s}(n)=\mathrm{sign}\left(\widehat{\mathcal{E}}_b(\Delta\tau)x_1(n,\Delta\tau)+\widehat{\mathcal{E}}_a(\Delta\tau)x_2(n,\Delta\tau)\right) \tag{34}$$

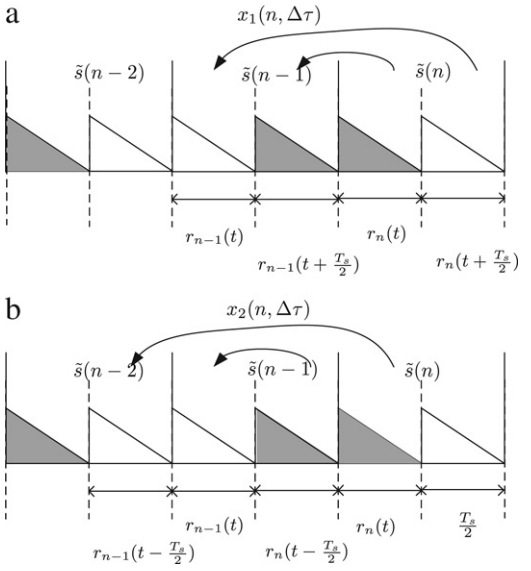

Fig. 5. Demodulation algorithm with a perfect timing synchronization.

and for $\Delta\tau \in [T_s/2, T_s)$

$$\widehat{s}(n)=\mathrm{sign}\left(\widehat{\mathcal{E}}_a(\Delta\tau)x_1(n-1,\Delta\tau)+\widehat{\mathcal{E}}_b(\Delta\tau)x_2(n,\Delta\tau)\right). \tag{35}$$

Comparison of these algorithms has been widely carried out in the literature (see e.g., [15,19,20]). It is well-known that MRC achieves the best performance by maximizing the SNR of the decision statistic. However, whether EGC or SC is better depends on the relative strength of $x_1(n,\Delta\tau)$ and $x_2(n,\Delta\tau)$. EGC will outperform SC when strength of $x_1(n,\Delta\tau)$ and $x_2(n,\Delta\tau)$ is comparable, and SC will perform better if one correlation function is much stronger than the other. A simple calculation will show that with uncorrelated, zero-mean and equal-variance noise, when the symbol strength of one correlation function is at least $(1+\sqrt{2})$ times that of the weaker one, SC will achieve a higher SNR and a better performance than EGC.

4.3. Special case: Perfect synchronization

The demodulator with perfect synchronization is a special case of the demodulation algorithm in the presence of mistiming. For perfect timing synchronization ($\Delta\tau = 0$), the extracted segments with index n are [cf. (24)] (see also Fig. 5)

$$\begin{aligned}r_n(t)&=\tilde{s}(n+1)R_j(t)+\eta_1(t)\\ r_n(t-T_s/2)&=\tilde{s}(n)R_j(t)+\eta_2(t)\\ r_n(t+T_s/2)&=\tilde{s}(n)R_i(t)+\eta_3(t)\end{aligned} \tag{36}$$

and segments with index $(n-1)$ are [cf. (25)]

$$\begin{aligned}r_{n-1}(t)&=\tilde{s}(n-1)R_i(t)+\eta_4(t)\\ r_{n-1}(t-T_s/2)&=\tilde{s}(n-2)R_i(t)+\eta_5(t)\\ r_{n-1}(t+T_s/2)&=\tilde{s}(n)R_j(t)+\eta_6(t)\end{aligned} \tag{37}$$

Please cite this article in press as: M. Ouertani, et al., Orthogonal bi-pulse UWB: Timing and (de)modulation, Physical Communication (2008), doi:10.1016/j.phycom.2008.10.001

where $r_{n-1}(t + T_s/2) = r_n(t - T_s/2)$, $i \neq j, i, j \in \{0, 1\}$ and $\eta_k(t)$ are noise terms. Note that, unlike (24) and (25) each segment in Eqs. (36) and (37) contains a complete $R_i(t)$, $i \in \{0, 1\}$, thanks to the perfect synchronization.

Using Lemmas 1 and 2, and the differential modulation relationship, we can simplify $x_1(n, \Delta\tau = 0)$ and $x_2(n, \Delta\tau = 0)$ as:

$$\begin{aligned} x_1(n, \Delta\tau = 0) &= 2s(n)\mathcal{E}_R + \xi_5(n) \\ x_2(n, \Delta\tau = 0) &= \xi_6(n) \end{aligned} \tag{38}$$

where $\mathcal{E}_R := \int_0^{\frac{T_s}{2}} (R_i(t))^2 \, dt$ for $i \in \{0, 1\}$, $\xi_5(n)$ and $\xi_6(n)$ are noise terms.

As shown in (38), correlation function $x_1(n, \Delta\tau = 0)$ captures the entire symbol energy. However, $x_2(n, \Delta\tau = 0)$ only consists of noise. So for this case, the optimal demodulation can be carried out in an SC manner by only using $x_1(n, \Delta\tau = 0)$ with a slicer,

$$\widehat{s}(n) = \text{sign}(x_1(n, \Delta\tau = 0)). \tag{39}$$

Under perfect synchronization, the symbol detector in (39) is simply a normal differential demodulator. Therefore, they are expected to achieve the same bit-error-rate (BER) performance. Of course, the correlation that generates the decision statistic $x_1(n, \Delta\tau = 0)$ differs from [2] and [11] due to the special bi-pulse modulation.

5. Simulations

In this section, we will evaluate the performance of our proposed approaches with simulations. We select the orthogonal pulses $p_0(t)$ and $p_1(t)$ as two consecutive order Hermite pulses with duration $T_p \approx 0.8$ ns. Simulations are performed in a modified Saleh–Valenzuela channel [16, 17] with parameters $\Lambda = 0.0233$ ns^{-1}, $\lambda = 2.5$ ns^{-1}, $\Gamma = 7.1$ ns and $\gamma = 4.3$ ns. The maximum channel delay spread is about 31 ns. Every symbol contains $N_f = 10$ frames each with duration $T_f = 32$ ns.

First, let us compare the acquisition probability of the proposed orthogonal bi-pulse TDT synchronizer with the original NDA and DA TDT algorithms in [1]. Thanks to the orthogonal pulses, the bi-pulse synchronizer remarkably outperforms the original NDA TDT algorithm and achieves a comparable performance to the DA TDT algorithm, especially when M is small (see Fig. 6).

In Fig. 7, we compare the mean square error (MSE) for all three TDT synchronizers. The MSE is normalized by the square of the symbol duration T_s. The performance of our bi-pulse IR in NDA mode is comparable to that of the original DA TDT synchronization algorithm. Even without any training symbol sequence, our bi-pulse TDT synchronizer can greatly outperform the original NDA TDT especially when M is small. This performance improvement is enabled at the price of slightly higher complexity by alternating the pulse shaper.

In Fig. 8, the BER performance associated with various TDT algorithms is tested, where M is the length of symbol sequence. Specially, the timing error is first estimated and corrected for the received signal. Then differential demodulation is carried out by assuming that the signal is perfectly synchronized. Our bi-pulse IR with NDA TDT can

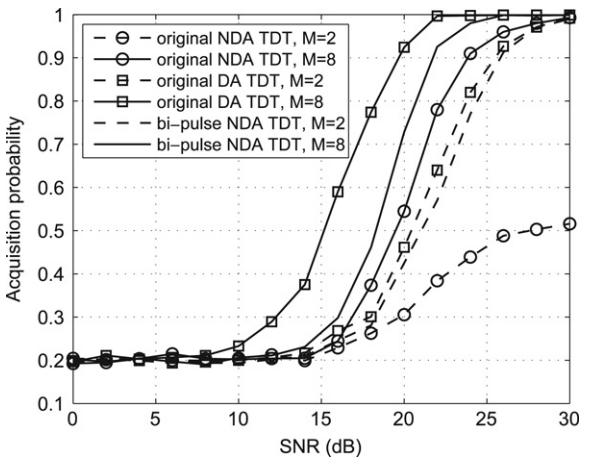

Fig. 6. Acquisition probability comparison: proposed TDT versus original DA and NDA TDT [1].

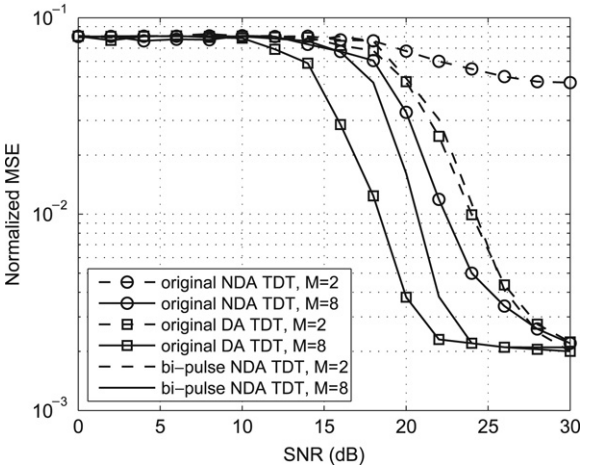

Fig. 7. MSE comparison: proposed TDT versus original DA and NDA TDT [1].

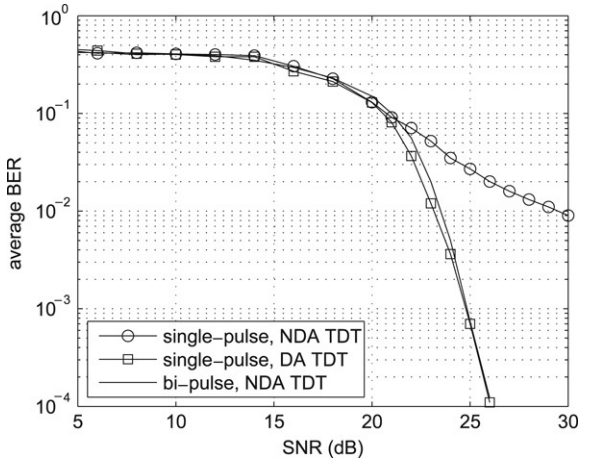

Fig. 8. Joint simulation of timing and demodulation for $M = 2$.

Please cite this article in press as: M. Ouertani, et al., Orthogonal bi-pulse UWB: Timing and (de)modulation, Physical Communication (2008), doi:10.1016/j.phycom.2008.10.001

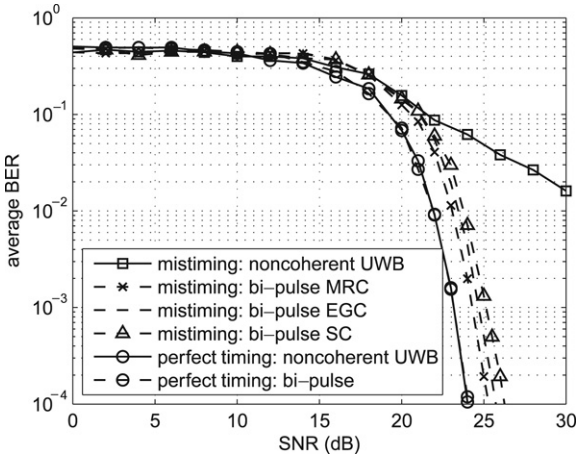

Fig. 9. Bi-pulse UWB versus noncoherent UWB [2]; timing error is in the range of $[0, T_s)$.

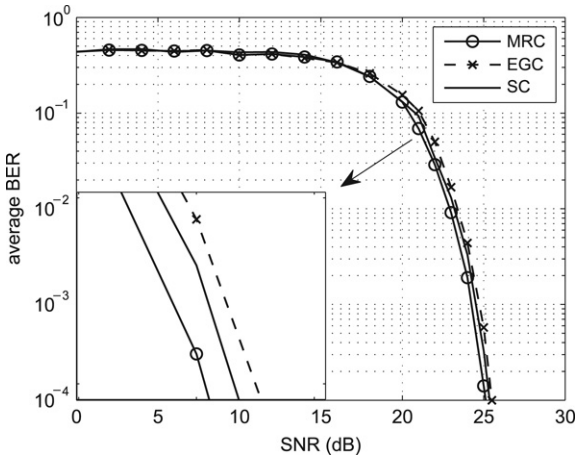

Fig. 10. Comparison of SC, EGC and MRC for bi-pulse UWB; timing error is in the range of $[0, T_f)$.

perform almost the same as the original IR with DA TDT and significantly outperform the original IR with NDA TDT. This is in accord with the simulation result that for $M = 2$, the timing performance of our bi-pulse system is similar to the original TDT in DA mode and much better than the original TDT in NDA mode (see Figs. 6 and 7).

In Figs. 9 and 10, we evaluate the BER performance of our proposed bi-pulse differential demodulator. We also compare the bi-pulse UWB with the original noncoherent UWB [2]. In the case of mistiming, the timing error is uniformly distributed in $[0, T_s)$ and $[0, T_f)$ for Figs. 9 and 10, respectively. From Fig. 9, we can see that when there is no mistiming, the bi-pulse noncoherent UWB achieves the same performance as the original noncoherent UWB. This is because with perfect timing, symbol detection of both is essentially differential UWB. By avoiding ISI, our bi-pulse noncoherent UWB leads to a simple demodulator with ML optimality even in the presence of unknown mistiming. However, under the same conditions, performance of original noncoherent UWB degrades drastically when Viterbi decoding is not used.

From both Figs. 9 and 10, we see that MRC outperforms EGC and SC in terms of BER. This has been well known because MRC can always maximize the SNR of the decision statistic. However, which of EGC and SC performs better depends on the range of timing error. For the small timing error range $[0, T_f)$, SC performs better (see Fig. 10). However, for the large timing error range $[0, T_s)$, EGC outperforms SC (see Fig. 9). This is because for the $[0, T_f)$ case, one of the two correlation functions almost contains the entire energy of the received symbol, but the other one is almost pure noise. By simply summing up these two terms, EGC actually suffers from an SNR degradation. For the $\Delta\tau \in [0, T_s)$ case, the energy contained in both two correlations is generally comparable. Although the stronger one is used for detection, SC still loses a large portion of the symbol energy. Therefore, EGC outperforms SC when the timing error is in a wider range of $[0, T_s)$, as shown in Fig. 9.

6. Conclusions

In this paper, we proposed a novel bi-pulse IR system, which employs a pair of orthogonal waveforms as pulse shapers in an alternating manner. Based on this system, we developed both a TDT-based timing synchronizer and a noncoherent demodulator. With the orthogonal bi-pulse modulation, our system can completely mitigate ISI in the correlation between adjacent half-symbol-long segments. As a result, our timing synchronizer can achieve a better acquisition performance than the original TDT synchronizer in NDA mode. For the same reason, our simple demodulator achieves ML optimality without the Viterbi decoding required by the original noncoherent UWB.

Acknowledgments

Work at the University of Florida is in part supported by Office of Naval Research under grant #N00014-07-1-0868.

Appendix. Proof of Lemma 1

Without loss of generality, we assume that the Hermite pulse $p_0(t)$ is evenly symmetric and $p_1(t)$ is oddly symmetric, both with respect to the origin [13]. Therefore, $p_0(t)$ and $p_1(t)$ are two orthogonal pulses.

Let $c(t)$ denote the real channel impulse response.[2] Then the received pulses corresponding to $p_0(t)$ and $p_1(t)$ can be expressed as $q_0(t) = c(t) * p_0(t)$ and $q_1(t) = c(t) * p_1(t)$. Next let us prove that $q_0(t)$ and $q_1(t)$ are two orthogonal pulses, which is equivalent to showing that

$$\int_{-\frac{T_p}{2}}^{\frac{T_p}{2}+T_h} q_0(t)q_1(t)\mathrm{d}t = 0 \tag{40}$$

where T_h is the excess delay spread of the channel.

[2] Note that $c(t)$ subsumes, but does not have to be, the tap-delay line model as in Eq. (3).

Please cite this article in press as: M. Ouertani, et al., Orthogonal bi-pulse UWB: Timing and (de)modulation, Physical Communication (2008), doi:10.1016/j.phycom.2008.10.001

Using Parseval's theorem, we can express the left hand side of (40) as

$$\int_{-\frac{T_p}{2}}^{\frac{T_p}{2}+T_h} q_0(t)q_1(t)\mathrm{d}t = \int_{-\frac{B}{2}}^{\frac{B}{2}} Q_0(f)Q_1^*(f)\mathrm{d}f \tag{41}$$

where $Q_0(f) = \mathcal{F}\{q_0(t)\}$ and $Q_1(f) = \mathcal{F}\{q_1(t)\}$ represent the Fourier transform for $q_0(t)$ and $q_1(t)$, z^* is the complex conjugate, and B is the bandwidth of the UWB pulse.

Due to the basic properties of Fourier transform with convolution operation, we have $Q_0(f) = C(f)P_0(f)$ and $Q_1(f) = C(f)P_1(f)$, with $C(f) = \mathcal{F}\{c(t)\}$, $P_0(f) = \mathcal{F}\{p_0(t)\}$ and $P_1(f) = \mathcal{F}\{p_1(t)\}$. Then (41) can be re-expressed as

$$\int_{-\frac{B}{2}}^{\frac{B}{2}} Q_0(f)Q_1^*(f)\mathrm{d}f = \int_{-\frac{B}{2}}^{\frac{B}{2}} P_0(f)P_1^*(f)|C(f)|^2\mathrm{d}f. \tag{42}$$

We know that if a function $f(t)$ is a real and even function, then its Fourier transform $F(f)$ is a real and even function; if $f(t)$ is a real and odd function, then $F(f)$ is a purely imaginary and odd function. Based on these, $P_0(f)$ turns out to be a real and even function, $P_1(f)$ is a purely imaginary and odd function, and $|C(f)|^2$ is a real and even function. Therefore, $P_0(f)P_1^*(f)|C(f)|^2$ is a purely imaginary and odd function. As a result, we have

$$\int_{-\frac{T_p}{2}}^{\frac{T_p}{2}+T_h} q_0(t)q_1(t)\mathrm{d}t = \int_{-\frac{B}{2}}^{\frac{B}{2}} P_0(f)P_1^*(f)|C(f)|^2\mathrm{d}f = 0 \tag{43}$$

which proves that $q_0(t)$ and $q_1(t)$ are orthogonal. In other words, the transmitted orthogonal pulses $p_0(t)$ and $p_1(t)$ remain orthogonal after propagating through a real channel, regardless of the multipath and possible inter-pulse interference.

References

[1] L. Yang, G.B. Giannakis, Timing Ultra-Wideband signals with dirty templates, IEEE Trans. Commun. 53 (11) (2005) 1952–1963.
[2] L. Yang, G.B. Giannakis, A. Swami, Noncoherent Ultra-Wideband (de)modulation, IEEE Trans. Commun. 55 (4) (2007) 810–819.
[3] K. Usuda, H. Zhang, M. Nakagawa, M-ary pulse shape modulation for PSWF-based UWB systems in multipath fading environment, in: Proc. of Global Telecommunications Conf., GLOBECOM, Dallas, TX, November 29–December 3, 2004, pp. 3498–3504.
[4] I. Dotlic, R. Kohno, Design of the family of orthogonal and spectrally efficient UWB waveforms, IEEE J. Sel. Top. Signal Process. 1 (1) (2007) 21–30.
[5] J.A. Ney da Silva, M.L.R. de Campos, Spectrally efficient UWB pulse shaping with application in orthogonal PSM, IEEE Trans. Commun. 55 (2) (2007) 313–322.
[6] L. Yang, G.B. Giannakis, Ultra-wideband communications: An idea whose time has come, IEEE Signal Process. Mag. 21 (6) (2004) 26–54.
[7] M.Z. Win, R.A. Scholtz, Impulse radio: How it works, IEEE Commun. Lett. 2 (1998) 36–38.
[8] M. Ouertani, H. Besbes, A. Bouallegue, Modified Hermite functions for designing new optimal UWB pulse-shapers, in: European Signal Processing Conference, EUSIPCO, Antalya, Turkey, September 4–8, 2005.
[9] X. Luo, L. Yang, G.B. Giannakis, Designing optimal pulse-shapers for ultra-wideband radios, IEEE J. Commun. Netw. vol. 5 (4) (2003) 344–353.
[10] C.K. Rushforth, Transmitted-reference techniques for random or unknown channels, IEEE Trans. Inform. Theory 10 (1) (1964) 39–42.
[11] M. Ho, V. Somayazulu, J. Foerster, S. Roy, A differential detector for an Ultra-Wideband communications system, in: Proc. of Vehicular Technology Conf., Birmingham, AL, May 4–9, 2002, pp. 1896–1900.
[12] M. Ouertani, H. Xu, L. Yang, H. Besbes, A. Bouallegue, A new modulation scheme for rapid blind timing acquisition using dirty template approach for UWB systems, in: Proc. of Intl. Conf. on Acoustics, Speech, and Signal Processing, Honolulu, HI, April 15–20, 2007, pp. III-265–III-268.
[13] L.B. Michael, M. Ghavami, R. Kohno, Multiple pulse generator for Ultra-Wideband communications using Hermite polynomial based orthogonal pulses, in: Proc. 2002 IEEE Conf. on Ultra Wideband Systems and Tech., Baltimore, MD, May 21–23, 2002, pp. 47–51.
[14] L. Yang, G.B. Giannakis, Optimal pilot waveform assisted modulation for Ultra-Wideband communications, IEEE Trans. Wireless Commun. 3 (4) (2004) 1236–1249.
[15] J. Proakis, Digital Communications, 4th ed., McGraw-Hill, New York, 2001.
[16] R.J.-M. Cramer, R.A. Scholtz, M.Z. Win, Evaluation of an Ultra-Wide-Band propagation channel, IEEE Trans. Antennas Propag. 50 (5) (2002) 561–570.
[17] A.A.M. Saleh, R.A. Valenzuela, A statistical model for indoor multipath propagation, IEEE J. Sel. Areas Commun. 5 (2) (1987) 128–137.
[18] T.P. Montoya, G.S. Smith, A study of pulse radiation from several broad-band loaded monopoles, IEEE Trans. Antennas Propag. 44 (8) (1996) 1172–1182.
[19] K. Sivanesan, N.C. Beaulieu, Exact BER analysis of bandlimited BPSK with EGC and SC diversity in cochannel interference and Nakagami fading, IEEE Commun. Lett. 8 (10) (2004) 623–625.
[20] M.K. Simon, M.S. Alouini, Digital Communication Over Fading Channels, Wiley, New York, 2000.

Mourad Ouertani received his Bachelor Degree in Mathematics in 2002, from the University of Sciences of Tunis, Tunisia, and Master and Ph.D. Degrees in Telecommunications from the National Engineering School of Tunis (ENIT), Tunisia, in 2003 and 2008, respectively. His research interests lie in signal processing and communication. Currently, he is focusing on synchronization techniques in UWB systems.

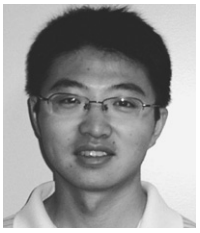

Huilin Xu received the B.Sc. and M. Sc. degrees from the University of Science and Technology of China (USTC), Hefei, China, in 2002 and 2005, respectively, both in Electrical Engineering. He is currently pursuing the Ph.D degree with the Department of Electrical and Computer Engineering, University of Florida, Gainesville, Florida. His research interests are in the areas of wireless communications and related fields.

Hichem Besbes was born in Monastir, Tunisia in 1966. He received his B.S. (with honors), M.S. degrees and his Ph.D. in Electrical Engineering from the Ecole Nationale d'Ingénieurs de Tunis' (ENIT) in 1991, and 1999, respectively. He has been with the Ecole Supérieure des Communications de Tunis (Sup'Com), as a lecturer during 1991–1999 and then as an assistant professor. From July 1999 to October 2000, he held a post-doctoral position at Concordia University, Montréal, Canada. In July 2001, he joined Legerity, Inc., Austin, Texas, USA, where he was a senior system engineer working on broadband modems. From March 2002 to July 2003, he was a member of Technical Staff at Celite Systems, Inc., Austin, Texas, where he contributed to definition, design, and development of Celite's high-speed data transmission systems over wireline networks, named Broadcast DSL. He is currently an associate professor at Sup'Com. His interests include signal processing for communication.

Please cite this article in press as: M. Ouertani, et al., Orthogonal bi-pulse UWB: Timing and (de)modulation, Physical Communication (2008), doi:10.1016/j.phycom.2008.10.001

Liuqing Yang (S'02-M'04-SM'06) received her B.S. degree in Electrical Engineering from Huazhong University of Science and Technology, Wuhan, China, in 1994, and her M.Sc. and Ph.D. degrees in Electrical and Computer Engineering from University of Minnesota, Minneapolis, in 2002 and 2004, respectively. Since August 2004, she has been an assistant professor with the Department of Electrical and Computer Engineering at University of Florida, Gainesville. Her current research interests include signal processing, communications theory and networking. Dr. Yang received the Best Dissertation Award in the Physical Sciences & Engineering from University of Minnesota in 2005, and the Office of Naval Research Young Investigator Award in 2007. She is the co-recipient of the Best Paper Award at IEEE international Conference on UWB (ICUWB) in 2006. She serves as an Associate Editor of the IEEE Transactions on Communications, IEEE Transactions on Wireless Communications, and IEEE Transactions on Intelligent Transportation Systems. She is also a member of the Editorial Board of Signal, Image and Video Processing Journal, and PHYCOM: Physical Communication. Dr. Yang serves as co-chair of the Mobile Communication Networks technical committee of the IEEE ITSS since 2006 and vice chair of the IEEE Gainesville section.

Ammar Bouallègue received the electrical engineering, and doctorate degrees from ENSERG de Grenoble, France, in 1971 and 1975, respectively, and docteur es-science degree from ENSEEIHT, INP de Toulouse, Toulouse, France, in 1984. In 1976, he joined the Ecole Nationale d'Ingénieurs de Tunis (ENIT), Tunisia. From 1986 to 1994, he was the head of the Electrical Engineering Department, ENIT, and from 1994 to 1996, he was the dean of Ecole Supérieure des Postes et des Télécommunications de Tunis, Tunisia. He is currently director of the research laboratory Communication Systems (Sys'Com) at ENIT. His research interests include information theory, channel coding, and signal processing for communication.

Please cite this article in press as: M. Ouertani, et al., Orthogonal bi-pulse UWB: Timing and (de)modulation, Physical Communication (2008), doi:10.1016/j.phycom.2008.10.001